

Free-space Beam Steering in Two Dimensions Using a Silicon Optical Phased Array

J. K. Doyle^{d*}, M. J. R. Heck, J. T. Bovington, J. D. Peters, L. A. Coldren, J. E. Bowers

Dept. of Electrical and Computer Engineering, University of California, Santa Barbara, California 93106, USA

**doylejd@ece.ucsb.edu*

Abstract: We report an independently tuned 16-channel optical phased array fabricated in silicon for 2D free-space beam steering. The phased array was composed of silicon-on-insulator waveguide surface gratings integrated with thermo-optic phase tuners and was operated both using a control algorithm together with automated real-time far field image analysis to target and shape the beam, and using a lookup table without real-time feedback. The device exhibited $1.6^\circ \times 0.6^\circ$ beam width and 10 dB background suppression in the far field across a $20^\circ \times 14^\circ$ field of view. We show that by increasing the waveguide width from 1 μm to 3 μm we can suppress the side-lobe peaks by a factor of 2.

OCIS codes: (060.2605) Free-space optical communication; (280.0000) LIDAR; (130.4815) Optical switching devices;

Sponsored By:

Defense Advanced Research Projects Agency, Microsystems Technology Office (MTO)

Program: CHip-scale Integrated Photonic Phased Array (CHIPPA), Issued by DARPA/CMO under Contract No. HR0011-10-2-0003.

The views and conclusions contained in this document are those of the authors and should not be interpreted as representing official policies of the Defense Advanced Research Projects Agency or the U.S. Government.

1. Introduction

Free-space optical chip-to-chip and board-to-board interconnects offer advantages with respect to packaging and density over waveguide-based approaches due to parallelism [1] and obviation of the need for fiber attachment. The capability to steer the beam is important for such applications and others such as optical scanning, LIDAR, crossconnect switching, and in order to prevent optical misalignment and hence increased insertion loss and crosstalk [2,3] from thermal or mechanical disturbances. Among the approaches used to accomplish chip-scale free-space beam steering are tunable gain elements [4], piezo-electric micro-stages [5], reconfigurable liquid-crystal phase gratings [6], MEMS microlenses [7] and micromirrors [8].

An approach that avoids mechanical motion can be advantageous in terms of robustness and susceptibility to vibration, while compatibility with standard CMOS silicon processing by fabricating the device in the silicon-on-insulator (SOI) platform is desirable for ease of fabrication and on-chip electronic integration. Furthermore such a platform allows the integration of the free-space beam steerer with tunable optical sources [9,10] and amplifiers [11] via hybrid integration of III-V materials with SOI optical waveguides. Optical phased arrays using surface waveguide gratings in SOI have been demonstrated using a combination of wavelength scanning and a single thermo-optic phase tuner for a steering range of $2.3^\circ \times 14^\circ$ [12,13], but suffered from the lack of a means to actively eliminate phase errors introduced by fabrication variation and thermal crosstalk. An alternate technique in which a star coupler was integrated with a grating array such that wavelength alone could be used to scan the beam across the far field was also demonstrated [14], thus eliminating the need for phase tuning altogether at the expense of beam width (4°) and the ability to actively shape the wavefront. Individually phase-tuning the channels in an SOI waveguide optical phased array solves these problems and has been demonstrated for 1D beam steering in a silicon slab [15]. Suppression of side-lobes in such a device is important both to direct a higher fraction of optical power into the central peak (thus enhancing efficiency) and to avoid optical crosstalk between adjacent free-space optical links.

We here report a 16-channel independently tuned optical phased array fabricated in SOI for 2D free-space beam steering over a $20^\circ \times 14^\circ$ field of view with $1.6^\circ \times 0.6^\circ$ beam width, and we investigate the effect of rib waveguide width on far field side-lobe suppression. The emission outcoupling angle was determined by wavelength in one axis and by relative phase between emitters in the other axis. Resistive heaters were used to phase-tune individual channels via the thermo-optic effect, and a hill-climber optimization algorithm together with real-time far field

feedback from an automated image analyzer was used to minimize phase errors and suppress background peaks. Solution sets were recorded for wavelengths from 1525 nm to 1625 nm, where a solution was defined by meeting the condition in which beam intensity exceeded the maximum background peak height by 10 dB for a field of view chosen so as to exclude the side-lobes. The recorded phase solutions were then used to steer the beam without real-time feedback using a lookup table.

2. Fabrication

Rib waveguides were photolithographically defined in 500 nm top silicon, 1 μm buried oxide SOI. The waveguides had 1 μm width and 280 ± 20 nm trench depth. The beam was separated into 16 channels spaced at 100 μm intervals using 1×2 multi-mode interferometers (MMI), and a separate phase tuning element was fabricated on each channel by e-beam deposition of 72 nm / 75 nm nickel-chrome/gold to form $470 \mu\text{m} \times 4 \mu\text{m}$ resistive heaters adjacent to each waveguide with a 6.5 μm separation to avoid metal optical absorption. The top silicon between adjacent channels was etched to the buried oxide so as to minimize thermal crosstalk. The grating array was fabricated with 50% duty cycle, 600 nm pitch and 200 μm length using e-beam lithography and etched 75 nm deep. Within the grating array the waveguide spacing was 3.5 μm ; this spacing determined the angular separation between the central peak and side-lobes, and hence the angle over which the beam could be swept without introducing side-lobes into the field of view. Waveguide widths within the grating array of 1 μm , 2 μm , and 3 μm were used to evaluate the effect of rib widths on the side-lobe peaks. Schematic diagrams of the device and a scanning electron microscope image of the grating array are shown in Figure 1.

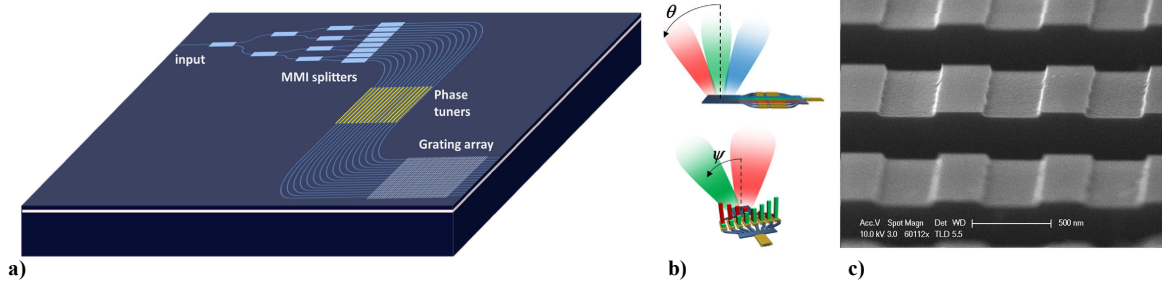


Fig. 1. a) Schematic diagram of the device. b) Illustration of the longitudinal θ emission angle determined by wavelength (top) and lateral emission angle ψ determined by phase (bottom). c) Scanning electron microscope image of the grating array.

3. Characterization

A high-numerical-aperture aspheric lens ($\text{NA} = 0.83$, effective focal length (EFL) = 15 mm) was used to collect the optical output and image it into the Fourier plane; two additional lenses (EFL 18 cm and 6 cm respectively) were used to image the Fourier plane onto an infrared camera for real-time far field imaging following the approach described in [16]. Polarization was aligned along the TE axis using a polarization controller. Beam steering in the longitudinal θ axis (i.e. the axis parallel to the waveguides) was determined by wavelength and measured to be $0.14^\circ/\text{nm}$ with a beam width (FWHM) of 0.6° for the 1 μm waveguide array, while steering in the ψ axis (i.e. the axis perpendicular to the waveguides) was determined by relative phase at the emitters.

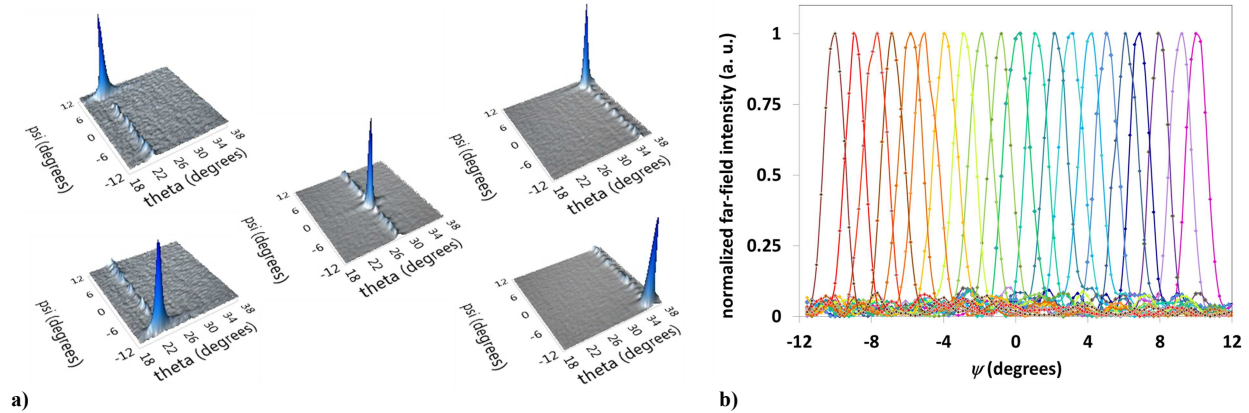


Fig. 2. a) Far field beam profiles for phase and wavelength set to steer the beam to the corners and center of the field of view. The low θ boundary (left) corresponds to emission at 1625 nm, the center corresponds to 1575 nm, and the high θ boundary (right) to 1525 nm. b) Cross sections in the ψ axis of the far field beam profile at 1555 nm for beam steering at 1° increments with 10 dB background suppression.

An optimization algorithm was used to solve for phase solutions with 10 dB background suppression within a 20° (ψ axis) \times 14° (θ axis) field of view at 1° increments. Once solved, these phase settings were stored in a lookup table and used to sweep the beam without real-time feedback. Measured profiles of the beam targeted to the corners and center of the field of view are shown in Figure 2(a); cross-sections of the beam in the ψ axis at a wavelength of 1555 nm are shown in Figure 2(b) for the 1 μm waveguide width array. Beam width in ψ was measured to be 1.6° .

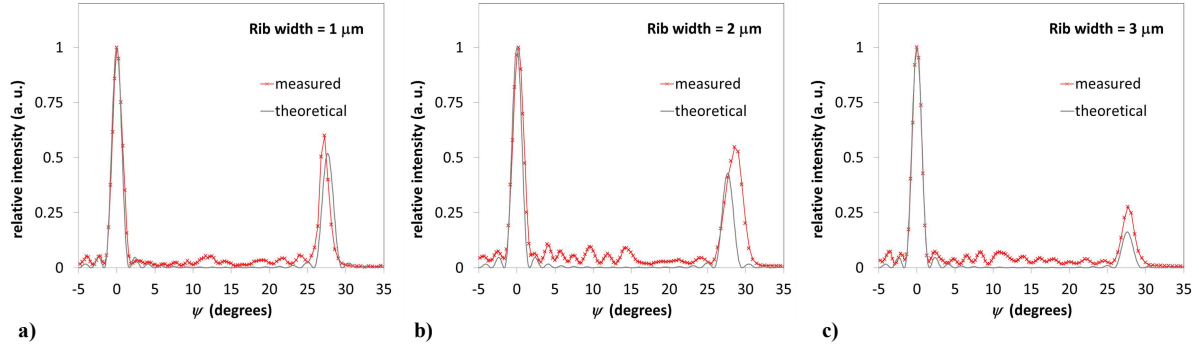


Fig. 3. Measured and calculated cross sections of the far field in ψ for 1625 nm wavelength showing the first side-lobe for a) 1 μm waveguide width, b) 2 μm waveguide width, and c) 3 μm waveguide width.

With waveguide spacing fixed at 3.5 μm , the relative power distribution in the side-lobes versus the central peak was determined by the emitter width, i.e. the rib waveguide width within the grating array. Measured and calculated cross-sections in ψ of the far field profile at 1625 nm are shown in Figure 3, where the calculated profile was determined by summing the far field contributions of emitter amplitudes corresponding to a cross-section at the grating etch depth (75 nm) of the fundamental mode for each waveguide width. As expected, side-lobe suppression improved for increased rib width, with side-lobe peak heights of 0.6, 0.55, and 0.28 relative to the central peak for rib widths of 1 μm , 2 μm and 3 μm respectively.

4. Summary and Conclusions

We have demonstrated a 16-channel optical phased array in silicon for 2D free-space beam steering with independently tuned channels. The device exhibited beam steering over a $20^\circ \times 14^\circ$ field of view with $1.6^\circ \times 0.6^\circ$ beam width and 10 dB background suppression. The effect of waveguide width on side-lobe suppression was investigated and found to decrease side-lobe peak power from 60% to 28% of the central peak height for waveguide widths ranging from 1 μm to 3 μm . This suggests that the efficiency of the optical phased array can be enhanced by optimizing the waveguide width.

5. References

- [1] L. J. Camp et al., "Guided-wave and freespace optical interconnects for parallel-processing systems: a comparison," *Appl. Opt.* **33**, 6168-6180 (1994).
- [2] V. N. Morozov et al., "Tolerance analysis for three-dimensional optoelectronic systems packaging," *Opt. Eng.* **35**, 2034-2044 (1996).
- [3] A. G. Kirk et al., "Design rules for highly parallel free-space optical interconnects," *IEEE J. Sel. Top. Quant. Electr.* **9**, 531-547 (2003).
- [4] N. W. Carlson et al., "Electronic beam steering in monolithic grating surface emitting diode laser arrays," *Appl. Phys. Lett.* **53**, 2275-2277 (1988).
- [5] M. Naruse et al., "Real-time active alignment demonstration for free-space optical interconnections," *IEEE Phot. Tech. Lett.* **13**, 1257-1259 (2001).
- [6] C. J. Henderson et al., "Free space adaptive optical interconnect at 1.25 Gb/s, with beam steering using a ferroelectric liquid-crystal SLM," *J. Lightwave Tech.* **24**, 1989-1997 (2006).
- [7] A. Tuantranont et al., "Optical beam steering using MEMS-controllable microlens array," *Sens. Actuators A, Phys.* **91**, 363-372 (2001).
- [8] D. M. Burns et al., "Optical beam steering using surface micromachined gratings and optical phased arrays," *Proc. SPIE* **3131**, 99-110 (1997).
- [9] A. W. Fang et al., "A Continuous Wave Hybrid AlGaInAs-Silicon Evanescent Laser," *IEEE Phot. Tech. Lett.* **18**, 1143-1145 (2006).
- [10] M. N. Sysak et al., "A hybrid silicon sampled grating DBR tunable laser," in *Group IV Photonics, 2008 5th IEEE International Conference on*, (Cardiff, Wales, 2008), pp. 55-57.
- [11] H. Park et al., "A Hybrid AlGaInAs-Silicon Evanescent Amplifier," *IEEE Phot. Tech. Lett.* **19**, 230-232 (2007).
- [12] K. Van Acoleyen et al., "Off-chip beam steering with a one-dimensional optical phased array on silicon-on-insulator," *Opt. Lett.* **34**, 1477-1479 (2009).
- [13] K. Van Acoleyen et al., "Two-dimensional optical phased array antenna on silicon-on-insulator," *Opt. Express* **18**, 13655-13660 (2010).
- [14] K. Van Acoleyen et al., "Two-Dimensional Dispersive Off-Chip Beam Scanner Fabricated on Silicon-On-Insulator," *IEEE Phot. Tech. Lett.* **23**, 1270-1272 (2011).
- [15] D. Kwong et al., "1 \times 12 Unequally spaced waveguide array for actively tuned optical phased array on a silicon nanomembrane," *Appl. Phys. Lett.* **99**, 051104 (2011).
- [16] N. Le Thomas et al., "Exploring light propagating in photonic crystals with Fourier optics," *J. Opt. Soc. Am. B* **24**, 2964-2971 (2007).